Unravelling flow dynamics and mixing efficiency in a cubic stirred tank

Anna Młynarczykowska[1*], *Klaudia* Zwolińska-Glądys[1] , *Marek* Borowski[1] and *Marek* Jaszczur[2]

[1]AGH University of Krakow, Faculty of Civil Engineering and Resource Management, Mickiewicza 30, 30-059, Kraków, Poland
[2]AGH University of Krakow, Faculty of Energy and Fuels, Mickiewicza 30, 30-059 Kraków, Poland

Abstract. Fluid mixing is essential in numerous industrial sectors, including chemical manufacturing, food processing, and wastewater management. Achieving effective mixing promotes uniform distribution of components, accelerates reaction kinetics, improves final product quality, and reduces operational energy consumption. The effectiveness of mixing operations is influenced by fluid properties, vessel geometry, and impeller design, which together determine flow patterns and mass transfer dynamics. In this research study, two jet-type impeller configurations were investigated in a cubic vessel through a combination of Computational Fluid Dynamics and Particle Image Velocimetry. The numerical models were validated against experimental measurements, allowing for the benchmarking of key indicators such as flow topology and mixing quality indices. The investigation covered multiple parameters, including impeller geometry and fluid properties. Two fluids with different viscosities were analyzed to assess the adaptability of each impeller design to varying different process conditions. The study emphasizes the influence of geometric and operational parameters on velocity distribution in a cubic stirred tank. The integrated experimental-numerical approach provided a comprehensive evaluation of hydrodynamic behavior, offering practical insight for optimizing energy-efficient mixing systems. The results demonstrated that impeller geometry substantially influences fluid motion, with a higher blade angle promoting more uniform mixing patterns, albeit at the cost of higher torque and energy demand.

1 Introduction

A mixing system consisting of a tank with a mechanical agitator is used in numerous processes across the chemical, biochemical, pharmaceutical, food, environmental engineering, mineral processing industries, and wastewater management. The optimal mixer component design, ensuring high mixing efficiency, is the most important factor influencing process costs and product quality. Therefore, knowledge of the velocity distribution and hydrodynamic behaviour of the mixed medium, as well as the energy requirements for a given tank-agitator configuration, is essential. For this purpose, different types of impellers are used to meet the specific requirements of a given mixing operation. Computational Fluid Dynamics (CFD) techniques have matured and now offer faster, more economical alternatives that reduce the need for extensive experimentation, relying instead on validation against experimental data.

Extensive research on conventional impellers, such as the Rushton turbine, has yielded a number of new designs that aim to improve the efficiency of this class of devices. These include widely used hollow-blade geometries such as the Chemineer CD-6 and the SCABA SRGT with concave blades, described by Van't Rietet et al. [1], Bakker et al. [2], and Nienow [3]. Nagata [4] experimentally investigated the effect of skewed-angle blades on the power coefficient for a two-blade rotor (PBT2) and found that this configuration exhibits lower energy consumption under efficient operating conditions. Suzukawa et al. [5] examined the effect of skewed blades on a four-blade rotor (PBT4) placed in a tank with baffles. Ammar et al. [6], using numerical modeling, assessed the effect of rotor design on the hydrodynamic structure of fluid motion generated by three different rotors: a six-blade flat-blade turbine, a Rushton turbine, and a turbine with skewed blades. They demonstrated that two Rushton turbines generated the greatest improvement in fluid circulation throughout the tank. Similar analyses were performed by Kumaresan and Joshi [7], indicating that blade shape can alter the fluid flow pattern and increase mixing intensity. They investigated the influence of rotor blade pitch angle on the flow and turbulence field, taking into account blade number, blade width and twist, blade thickness, and pumping direction, using various rotor geometries. Driss et al.[8], on the other hand, used numerical calculations to analyse the energy consumption caused by changing the turbine blade pitch angle for 45°, 60°, and 75° pitch

* Corresponding author: mindziu@agh.edu.pl

settings. The results show that the power number decreases with decreasing pitch angle at a fixed Reynolds number. Similar conclusions were drawn by Chapple et al. [9], who examined the effect of blade thickness and rotor diameter on energy consumption, indicating that changes in rotor position can significantly impact the power number. Ameur and Bouzit [10] evaluate the influence of rotor clearance, blade diameter, vessel base shape, and blade bottom shape on hydrodynamic behaviour and shear rate distributions. They also analysed the influence of rotor speed, fluid rheology, and rotor blade curvature on mean velocities and energy consumption. They found that a flat-bladed turbine achieved the best efficiency at high Reynolds numbers, but incurred higher energy consumption compared with a curved-bladed rotor. Aubin et al. [11] used the Laser Doppler Velocity technique for a PBT turbine to map the turbulent flow field and quantify the required energy. They showed that upward pumping (flow directed above the impeller) yields lower flow rates and consumes more energy than downward pumping. Similarly, Ameur et al. [12] numerically studied the effect of several design parameters on the flow energy efficiency and energy consumption for a Maxblend impeller, an anchor impeller, a valve impeller, and twin-screw ribbon impellers. They found that the Maxblend impeller provided the best mixing performance.

Results obtained from numerical calculations (CFD) require experimental validation of the flow field. A commonly used technique is Particle Image Velocimetry (PIV). Ben Amira et al. [13,14] used PIV to determine the flow fields generated by an eight-bladed turbine with variable blade pitch. They demonstrated the direct effect of rotor geometry on the magnitude and direction of the velocity vectors. Similar experiments were performed by Jing et al. [15] to investigate the effect of blade shape on vorticity in turbulent fluid flow through four different disc rotors, including a Rushton-type rotor, a disc rotor with concave blades, a disc rotor with semi-elliptical blades, and a disc rotor with parabolic blades. The results showed that increasing blade curvature reduces the inclination of the jet ejected from the impeller region and weakens the radial jet. The widespread use of disc rotors or other types of turbines often fails to meet operational requirements, especially when mixing high-viscosity fluids or when a single impeller must perform across a broad range of fluid viscosities. Varying fluid viscosity poses complex challenges that require impeller designs optimized for both hydrodynamic performance and operational efficiency. Młynarczykowska et al. [16,17] conducted experimental studies comparing different impeller geometries to evaluate mixing times and flow patterns across a wide viscosity range. They confirmed that optimized impeller shapes can improve performance in stirred tanks, particularly as fluid viscosity increases. Similarly, Zhang et al. [18], Zhan et al. [19], and Liyanage et al. [20] showed a clear relationship between fluid viscosity and mixing efficiency, and they reported the superiority of proposed innovative impeller designs over conventional turbines in terms of process efficiency and reduced energy use. Prajapati [21] also identified the optimal number of blades for two- and four-blade anchor impellers designed for mixing pseudoplastic fluids.

The main challenge, therefore, is to develop a new blade design that can improve pumping capacity and reduce the energy use of the process. CFD modelling combined with experimental studies using PIV offers an effective approach to developing efficient mixing technologies suitable for fluids with variable viscosity.
As the cited studies indicate, the key factors influencing the efficiency of a mechanical mixing process, reducing energy consumption while ensuring product quality, are the shape and orientation of the mixing elements (blades). A literature review also reveals that relatively few studies have addressed mixing in cubic tanks. These tanks are becoming increasingly common in both transportation and production, and they require impeller geometries different from those offered for cylindrical vessels. The main differences between mechanical mixing in a cubic and cylindrical tank concern the symmetry of the velocity field, the distribution of dead zones, and the influence of corners and boundary conditions. This translates into different meshing requirements and turbulence models in CFD, as well as optical and calibration challenges for PIV measurements. The corners of a cubic tank create either dead zones or local recirculation zones and strong shear gradients. This changes the mixing and suspension effects of particles and makes it difficult to generalize results or compare them between geometries. For a cubic tank, local mesh refinements at corners and edges and the use of advanced turbulence models are recommended. However, this approach generates high computational costs.

Therefore, this study, as part of the development and verification of prototype impeller designs, presents the results of a flow pattern and energy consumption analysis, as well as experimental measurements of an innovative jet impeller in a cubic tank. For this purpose, advanced computational fluid dynamics and particle image velocity measurements were employed. Mixing efficiency was assessed by analysing the fluid motion and measuring torque while systematically varying impeller geometry, rotational speed, and fluid viscosity.

2 Methods

2.1. Test set-up and settings

The research study was divided into four stages. The procedure is presented in Figure 1. The initial stage involved conceptual work to define the objectives. The second stage consisted of experimental measurements, enabling the determination of velocity fields and a detailed analysis of mixing characteristics. Subsequent steps comprised numerical simulations for selected impeller geometries as part of a preliminary analysis of the mixing process. Depending on the results, individual stages were iterated to obtain optimal rotor configurations for the experimental verification stage. Ultimately, based on these findings, the power number

(Np) and the operational efficiency of the innovative jet impeller in a cubic tank were determined.

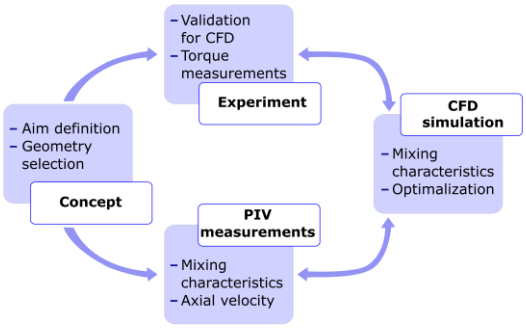

Fig. 1. Conceptual research workflow.

Flow fields were obtained using Computational Fluid Dynamics and Stereoscopic Particle Image Velocimetry (Stereo PIV) measurements, while the power consumption was measured using a precise torque meter. The experimental setup consisted of a cubic tank and a mechanically driven agitator coupled to an electric motor with continuous speed control. As working fluids water (ρ = 998.2 kg/m3, μ = 1.01 mPa·s at 20°C) and glycerine (ρ = 1261.1 kg/m^3, μ = 949 mPa·s at 20°C) were used. The impeller was mounted at the end of the shaft and at a specified height above the tank bottom. In all tests, the impeller axis was positioned at one-third of the fluid height ($h=1/3H$).
The geometry of the tested rotors is shown in Figure 2. The innovative rotors are scaled-down reproductions of a proposed industrial design, fabricated by 3D printing, and have smooth plastic walls of a thickness of 2 mm. The impeller is named Jet-1 uses bucket-shaped arms as the mixing element instead of conventional blades, while Jet-2 features similar bucket-shaped arms with symmetrically arranged slots.

(a) (b)

Fig. 2. Geometry of the tested impellers: Jet-1 (a), Jet-2 (b).

Torque was measured using a torque meter FSA-2 (AXIS, max 2 N·m) with an accuracy of 0.001 (N·m) and a sampling frequency of 1000 Hz. Figure 3 shows a schematic diagram with the dimensional annotations.
A summary of the tank and impellers dimensions is presented in Table 1.

Table 1. Dimensions of the tank and impellers.

Parameter	Symbol	Value, mm
Height of the tank/fluid	H_c / H	500 / 300
Width of the tank	a	300
Impeller distance from bottom	h	100
Diameter of the impeller	d	140
Length of the bucket	l	50
Diameter of the bucket's	w_1 / w_2	31.0 / 16.5

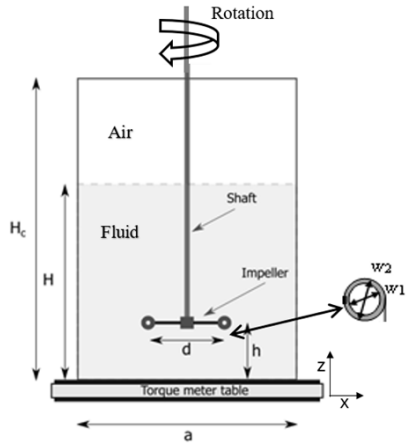

Fig. 3. Schematic of the experimental set-up Jet impeller.

Additionally, Figure 4 shows the Stereo-PIV set-up during operation with the Nd:YAG (400mJ) laser.

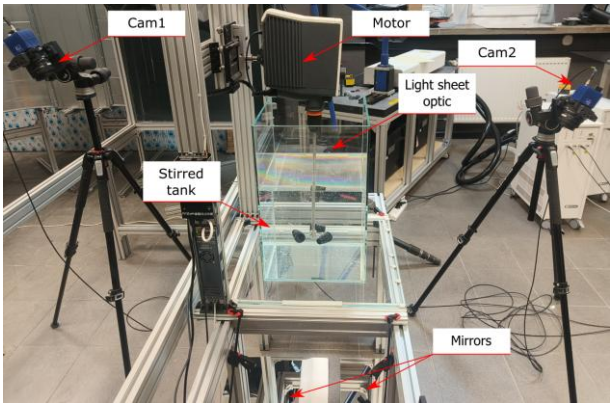

Fig. 4. View of the Stereo-PIV test stand.

Measurements of the torque required to rotate the impeller (and thus generate flow in the tank) were recorded for variable impeller geometry, including different inclination angles of the buckets. From the tested configurations, three bucket orientations were selected for detailed studies: 0° (buckets in the impeller plane), +15° (buckets inclined upwards), and -15° (buckets directed downwards). The impeller rotational speed of the impeller was varied in the range from 20 to 500 rpm. In addition to assessing the effect of geometry on mixing efficiency, the influence of nozzle tilt angles on this factor was also analyzed.

The mixing process characteristics on the prepared test rig were analyzed using the Stereo-PIV method (see Figure 4), which includes two cameras, Imager CX12 from LaVision (12-bit, 4080 × 2984 pixels), each equipped with a 50-mm/1.8 lens. A detailed description of the measurement procedure and validation of the stand is provided in [22-24]. To process the time series of image pairs and to evaluate all components of the velocity vector, DaVis software version 11.2 was used [25].

2.2 Calculation procedure based on experimental results

The experimental data were post-processed in order to evaluate the performance of the proposed solutions.

Among the most frequently used parameters for the mixing systems are the power number *Np* and pumping capacity Q_z Both criteria are typically presented as a function of the Reynolds number:

$$Re = \frac{nd^2\rho}{\mu} \quad (1)$$

where ρ is the density (kg/m^3), μ is the dynamic viscosity (kg/m·s), n is the rotational speed (rot/s), and d is the diameter of the impeller (m).

The power number *Np* can be determined using the formula:

$$N_p = \frac{P}{\rho n^3 d^5} \quad (2)$$

The power P required to rotate the impeller at a given rotational speed depends on the torque τ and is calculated as follows:

$$P = 2\pi \cdot n \cdot \tau \quad (3)$$

In order to determine the pumping capacity, the axial velocity component was calculated. For various Reynolds numbers, the axial velocity field was evaluated on a horizontal plane located midway between the bottom of the tank and the impeller (z = 50 mm). The pumping capacity was calculated from the Stereo-PIV measurements by integrating the mean absolute axial velocity over the horizontal radial positions below the rotor, i.e., between radial positions r_1 = 0.0 mm to r_2 = 70.0 mm

$$Q_z = \int_{r_1}^{r_2} |u_z| dS \quad (4)$$

This parameter is also commonly presented in a dimensionless form:

$$Q_{z,norm} = \frac{Q_z}{nd^3} \quad (5)$$

The determined values of this parameter were used to compare rotors of different shapes under turbulent flow conditions

2.3 Mathematical and Numerical Modelling

The mechanically agitated vessel configuration, as shown in Figure 1, served as the reference for comparative simulations. The steady state flow inside the stirred tank was described by governing equations for mass and momentum conservation

$$\frac{\partial u_i}{\partial x_i} = 0 \quad (6)$$

$$\rho u_j \frac{\partial u_i}{\partial x_j} = -\frac{\partial p}{\partial x_i} + \frac{\partial}{\partial x_j}\left[\mu\left(\frac{\partial u_i}{\partial x_j} + \frac{\partial u_j}{\partial x_i}\right) - \rho\overline{u_i' u_j'}\right] \quad (7)$$

The last term in eq. (7) introduces additional unknowns that require a turbulence model for closure. To determine the value of the Reynolds stress [26], the *k-ε* turbulence model, was employed:

$$\frac{\partial}{\partial x_i}(\rho k u_i) = \frac{\partial}{\partial x_j}\left[\left(\mu + \frac{\mu_t}{\sigma_k}\right)\frac{\partial k}{\partial x_j}\right] + G_k - \rho\varepsilon \quad (8)$$

$$\frac{\partial}{\partial x_i}(\rho \varepsilon u_i) = \frac{\partial}{\partial x_j}\left[\left(\mu + \frac{\mu_t}{\sigma_\varepsilon}\right)\frac{\partial \varepsilon}{\partial x_j}\right] + C_{1\varepsilon}\frac{\varepsilon}{k}G_k - C_{2\varepsilon}\rho\frac{\varepsilon^2}{k} \quad (9)$$

where,

u_i, is the velocity component respectively, in the i, j and z direction and

$$\mu_t = \rho C_\mu \frac{k^2}{\varepsilon} \quad (10)$$

where, G_k is the generation of k due to mean velocity gradients and μ_t represents the turbulent viscosity.
The constant values used for that model are: $C_{1\varepsilon}$=1.44, $C_{2\varepsilon}$ =1.9, C_μ=0.09, σ_k=1 and σ_ε=1.2.
Set of eq. (6)-(10) consists of 6 equations that need to be discretized and solved numerically. Ansys Fluent was used as a solver. Mesh independence tests were performed during the validation phase, and a grid independence was established. The final mesh used a medium resolution consisting of approx. 1600000 quad dominant control elements (Fig. 5).

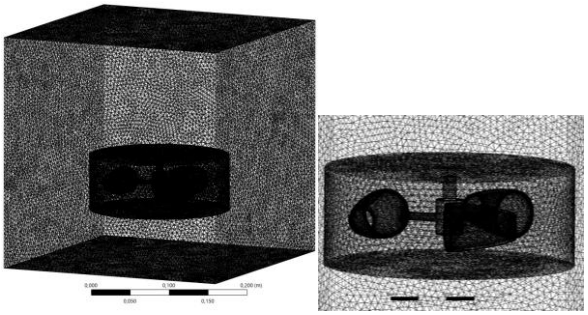

(a) (b)

Fig. 5. Mesh of the computational domain for numerical analysis: outside (a) and in the impeller zone (b).

3 Results and discussion

The primary objective of this study was to evaluate the influence of impeller geometry, inclination angle, and fluid viscosity on the mixing system efficiency

This required a detailed analysis of flow patterns, energy consumption, as well as experimental measurements (like impeller torque) for the innovative jet-type impeller located in a cubic tank. Computational fluid dynamics and particle image velocity measurements were employed to provide complementary datasets for validation and performance assessment.

3.1 Simulation results and torque measurements

The main goal in this study, as in any industrial process, has been to find the optimal configuration mixer system for an efficient mixing process using the lowest possible power.
During the mixing tests for Jet-1 and Jet-2 impellers, the torque was both experimentally measured and numerically predicted as the key parameter describing the hydrodynamic performance of the mixing process. Figures 6 and 7 present the results obtained for both impeller geometries, considering various bucket blades inclination angles. In each case, the rotational speed resulted in a proportional increase in torque, reflecting the higher hydrodynamic resistance experienced by the impeller. An additional factor contributing to torque

growth was the high viscosity and density of the working fluid (see Figure 7).

The simulation data in Figures 6 and 7 show that for Jet-1 and Jet-2 with an inclination of +15˚ are consistent with the experimental data. The lowest torque values were recorded for the Jet-1 impeller (+15°), indicating a favourable fluid circulation pattern inside the tank. For this turbine, the other tested configurations generated higher flow resistances, resulting in approximately 20% higher torque values, particularly noticeable at rotational speeds above 250 rpm

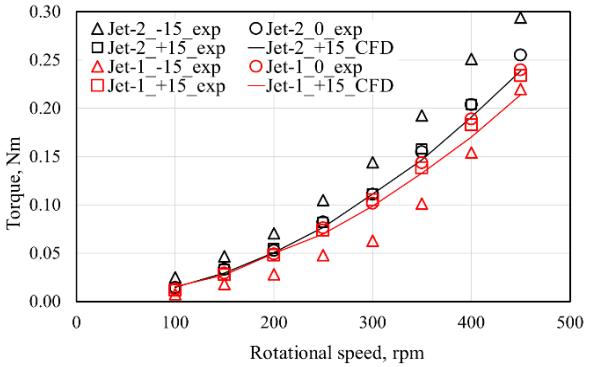

Fig. 6. Torque as a function of rotational speed for water for each inclination –Jet-1 and Jet-2.

For the Jet-2 rotor, the least favourable bucket inclination, the angle (+15°), created the highest torque, especially above 200 rpm, where torque values were 25% to 50% higher than for other configurations.
Direct visualisation also confirmed intense turbulent and vortex formation along the stator at a rotational speeds exceeding 400 rpm. A similar torque trend was observed for glycerine, as illustrated in Figure 7.

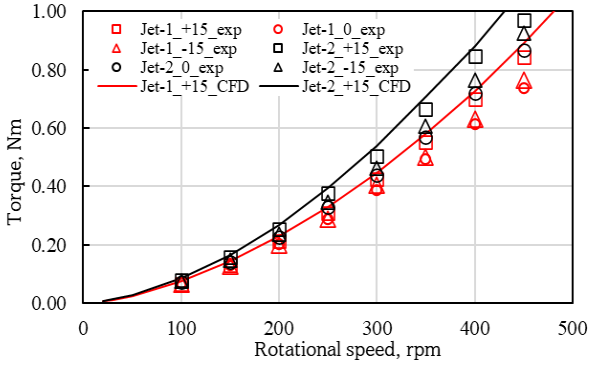

Fig. 7. Torque as a function of rotational speed for glycerine for each inclination –Jet-1 and Jet-2.

Based on the results, it can be indicated that the lowest flow resistance occurred at low rotational speeds (50-200 rpm), where torque values were comparable across all configurations. Therefore, the highest torque values were recorded for rotor speeds above 250 rpm when the Jet-2 rotor buckets were set at an angle (+15°). It should be noted that the CFD predictions for both fluids deviated by less than 5% from the experimental results, confirming the high accuracy and reliability of the numerical model. These impellers have the potential for energy-efficient industrial mixing applications

3.2 Mixing process performance

Based on experimental measurements (including PIV) the pumping capacity Q_z and power number N_p, were calculated and are shown in Figures 8 and 9 as a function of the Reynolds number. To compare the mixing efficacy and energy requirements for the individual impeller geometries analyzed, the determined values were presented in normalized and dimensionless form. Figure 8 presents the Power number *Np* for both innovative impellers.

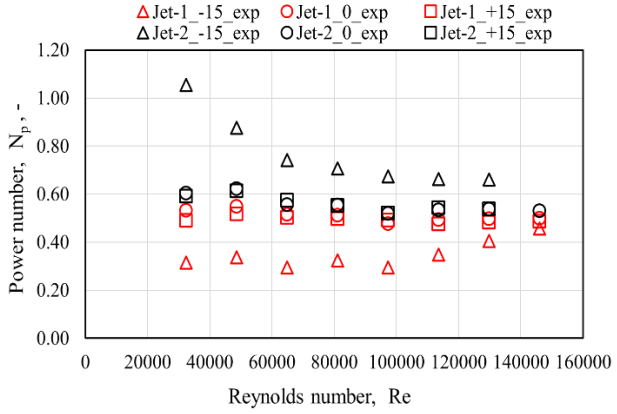

Fig. 8. Power number N_p for Jet-1 and Jet-2 impellers operating in water.

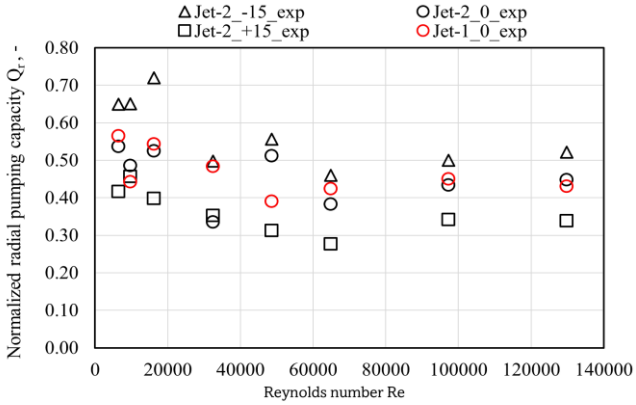

Fig. 9. Non-dimensional radial pumping capacity for the proposed impeller Jet-2 and Jet-1 (0) in water.

The Jet-1 impeller (-15°) exhibited the highest energy requirement under mixed flow conditions, whereas the Jet-2 impeller (-15°) demonstrated approximately 70% lower energy consumption while maintaining strong pumping capacity. For the remaining configurations, a stable and low-power number was observed, along with adequate liquid mixing capacity, especially in highly turbulent flows. As shown in previous studies (see Chapter 1 and [22]), the Rushton turbine is referred to as a reference impeller, providing efficient mixing with moderate energy. Its dimensionless pumping number (Q_r) o constant over a wide range of rotor speeds (above N = 500 rpm). In contrast, the Jet-1 and Jet-2 impellers achieved up to tenfold lower power N_p number compared to the Rushton turbine and other commonly used radial or mixed flow impellers.

3.3 Flow patterns study - PIV

A detailed examination of the flow behaviour during the mixing process was conducted based on the analysis of the Stereo Particle Image Velocimetry results. The investigation primarily focused on the velocity fields beneath the impeller for both geometries, aiming to assess the influence range of individual rotors as a function of configuration and rotational speed. Particular attention was devoted to both the magnitude and spatial distribution of velocities across the entire horizontal control plane. Figures 10 and 11 present the velocity fields obtained below the impellers operated in water at a rotational speed of 200 and 400 rpm.

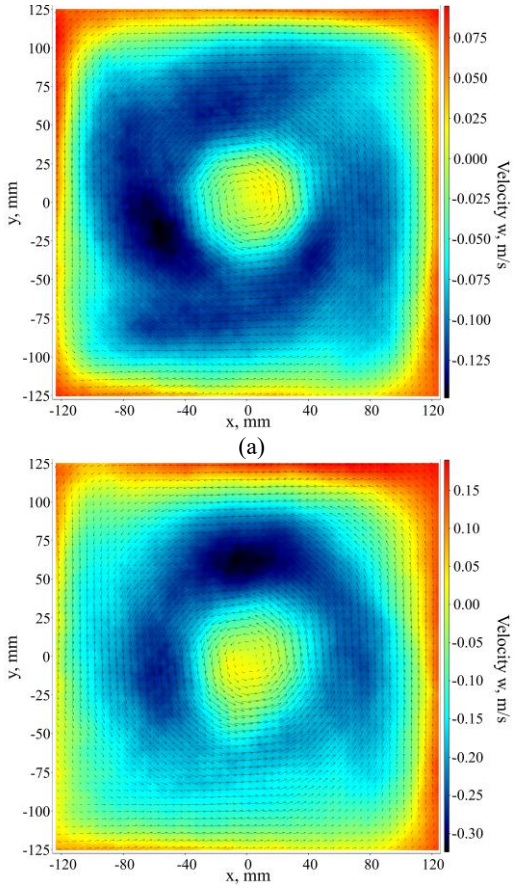

(a)

(b)

Fig. 10. Vertical component of velocity in the *xy* plane for inclination 0˚Jet-1 plane for rotational speed: (a) *N*=200 rpm, (b) *N*=400 rpm**.**

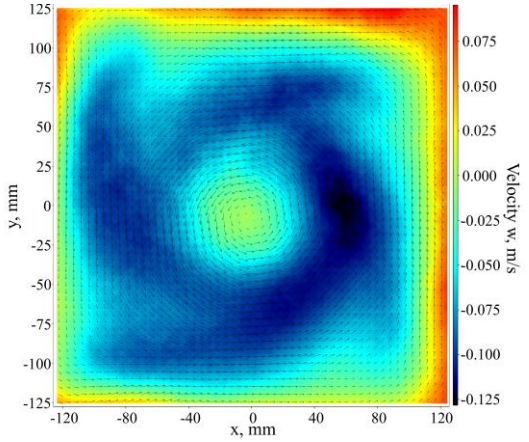

(a)

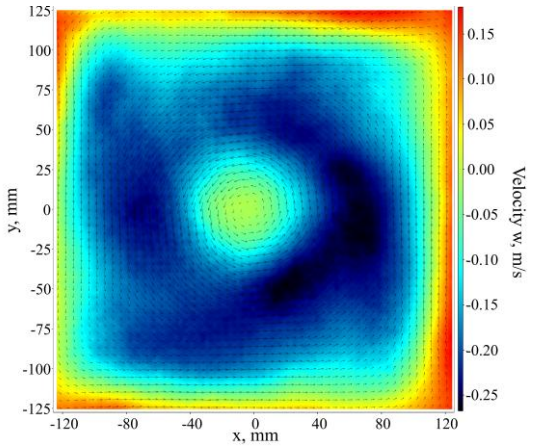

(b)

Fig. 11. Vertical component of velocity in the *xy* plane for inclination 0˚Jet-2 plane for rotational speed: (a) *N*=200 rpm, (b) *N*=400 rpm.

When comparing the velocity field plots for the individual impellers, similarities can be identified beyond the effects of rotational speed, with this trend being particularly evident for the Jet-2 impeller. The Jet-1 geometry promotes the formation of more circular regions of elevated velocity in the central part of the plane, whereas Jet-2 directs the flow more prominently toward the corners of the tank. For a given rotational speed, the vertical component of velocity ranges are comparable at lower speeds. However, at higher rotational speeds, the Jet-2 impeller generates noticeably lower velocity values. Moreover, a more uniform velocity distribution across the test plane is observed for Jet-2, with minimal localized deviations.

The subsequent stage of the analysis focused on examining the influence of impeller inclination on the velocity distribution within the analyzed plane. A higher rotational speed of 400 rpm was selected for this investigation. Specifically, the distribution of the vertical velocity component beneath the Jet-2 rotor was analyzed for inclination angles of −15° and +15°, respectively. The corresponding results are presented in Figure 12.

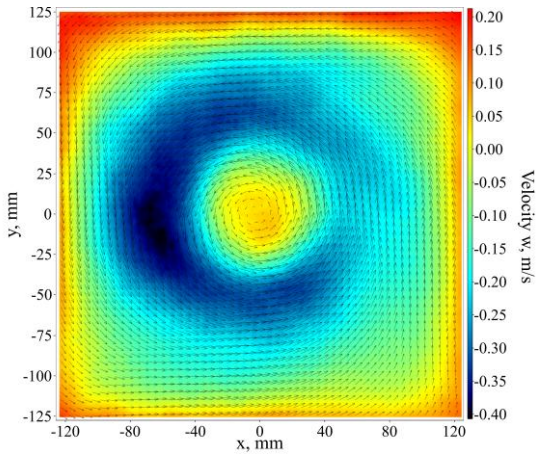

(a)

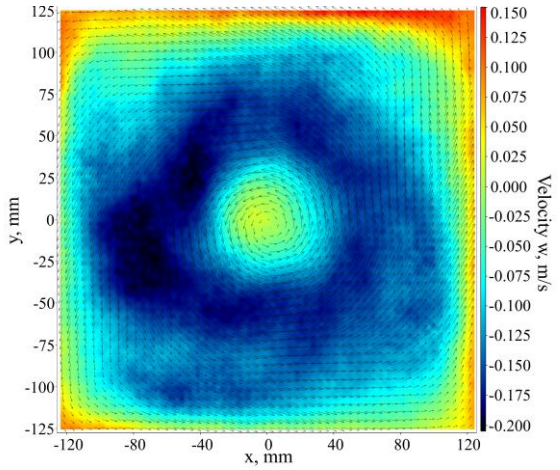

(b)

Fig. 12. Vertical component of velocity in the xy plane for Jet-2 with rotational speed N=400 rpm and inclination: (a) -15˚, (b) +15˚.

The results indicate that an inclination of −15° enables significantly higher downward water flow toward the bottom of the reservoir, reaching velocities of up to 0.40 m/s. In comparison, the maximum velocities for the non-inclined and +15° configurations were approximately 0.25 m/s and 0.20 m/s, respectively. A positive inclination of +15° also induces local turbulence and flow dispersion, which may contribute to a reduction in overall flow velocity. Overall, the findings suggest that the Jet-2 impeller inclined at −15° demonstrates notably favourable flow characteristics.
The authors in [24] presented the mean velocity fields for both rotors without tilt (0˚) and with tilt +15˚ for the selected rotational speed, obtained from SPIV measurement. Additionally, in chapter 3.4, to illustrate the liquid flow in the vessel, example flow pattern for the tested Jet-1 impeller are presented.

3.4 Flow patterns study – CFD

In order to reveal the influence of fluid viscosity on mixing efficiency by evaluating the velocity distribution, Figures 13 and 14 present velocity field images for the Jet-1 impeller over a wide range of impeller speeds. Figure 13 shows the velocity magnitude contour for Jet-1 impeller at rotational speeds N = 200, 400 rpm in the xy cross-section plane for z = 7 cm from the bottom of the tank.

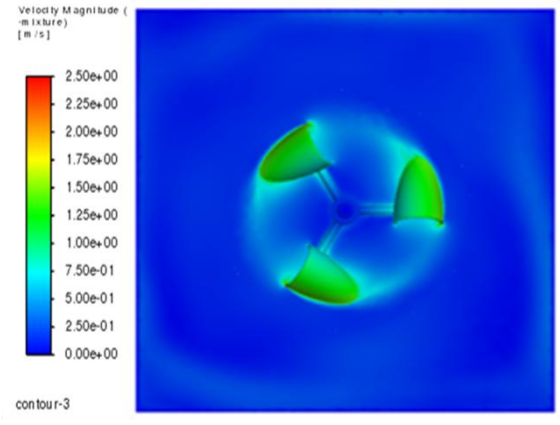

(a)

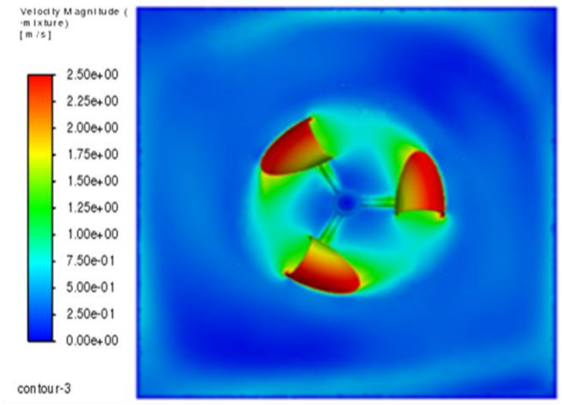

(b)

Fig.13. Mean velocity field for water and rotational speed N=200 (a), 400 (b) rpm. Jet-1 (+15˚) in the xy plane.

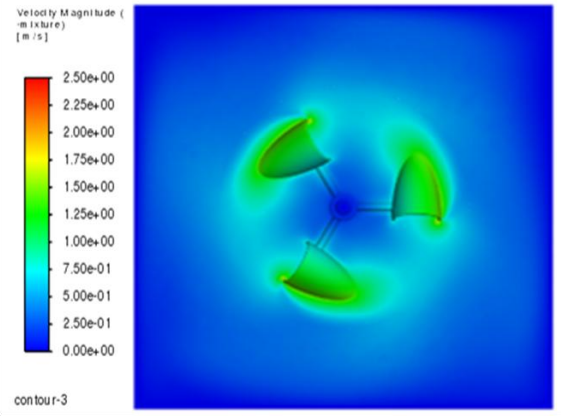

(a)

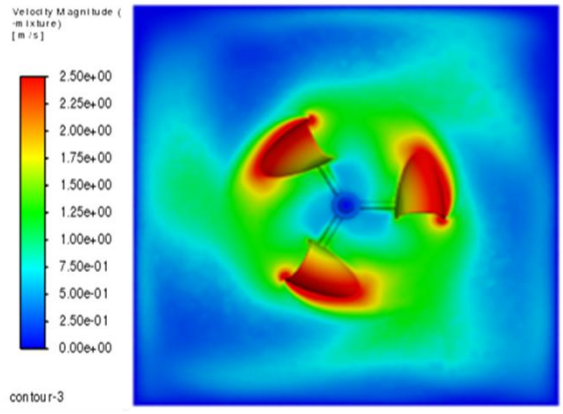

(b)

Fig. 14. Mean velocity field for glycerine and rotational speed N=200 (a), 400 (b) rpm. Jet-1 (+15˚) in the xy plane.

One may infer from this figure a high-velocity magnitude in the internal part of the impeller channel type bucket-blades. The fluid entering the bucket is directed upward while exiting through the smaller outlet opening. As a result, as the rotational speed increases, a zone of intense mixing is created around the impeller (Jet-1), revealed by the increasing velocity field of fluid. For low-viscosity fluids (water), the area of most intense mixing is concentrated around the Jet-1 and is limited by its diameter. In the case of glycerine, the fluid motion zone expands beyond the rotor already at N = 200 rpm and continues to expand as the rotational speed increases. This allows the fluid to be mixed throughout almost the entire volume of the tank. It should be noted that high fluid viscosity and high rotational speed can

cause the medium's temperature to increase over time. The temperature measurement taken after a series of experiments showed an average increase of 1 degree within 6 hours.

Figure 15 presents a comparison of the velocity fields obtained for Jet-1 and Jet-2 impellers used to mix fluids in a wide range of viscosities (water and glycerine). The analysis of the obtained images indicates that the Jet-2 rotor generates results analogous to the Jet-1 rotor under established hydrodynamic conditions. However, it should be noted that the presence of symmetrical holes on the walls of Jet-2 buckets causes the formation of additional small vortices in the immediate vicinity of the surfaces of the mixing elements. The additional fluid movement is more clearly visible in the inner zone of the rotor and the narrower part of the bucket. The fluid is directed downwards through the outlet hole, and during its movement, it may encounter another impeller bucket raised upwards. However, part of the stream passes below the rotor. Due to this movement of the fluid, the resistance to movement is reduced (lower energy demand), but the mixing efficiency does not increase significantly (see Figures 8 and 9)

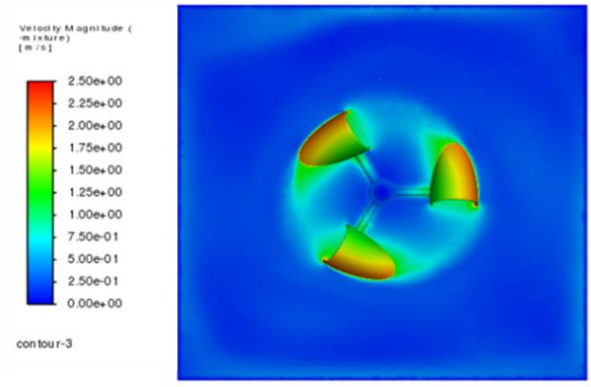

(a)

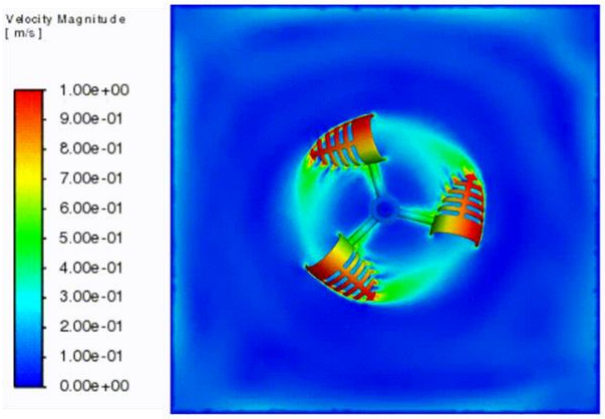

(b)

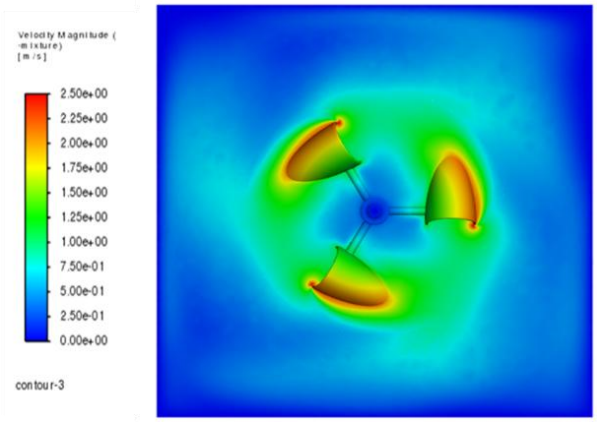

(c)

Fig. 15. Mean velocity field for *N*=300 rpm rotational speed, for: (a) Jet-1 (+15˚), (b) Jet-2 (+15˚) in water,(c) Jet-1 (+15˚) in glycerine,.

Furthermore, as a supplement to the SPIV results (see Section 3.3), Figure 16 presents selected flow patterns for the Jet-1 impeller, illustrating the fluid motion during mixer operation. The results obtained with water as the working fluid in varying rotational speeds indicate a circulating fluid flow below the impeller. This condition results from the coexistence of axial and radial fluid motion. These intense flows can have a decisive impact on the quality effect of the overall process. A detailed analysis of changes in flow patterns will be presented in a separate paper.

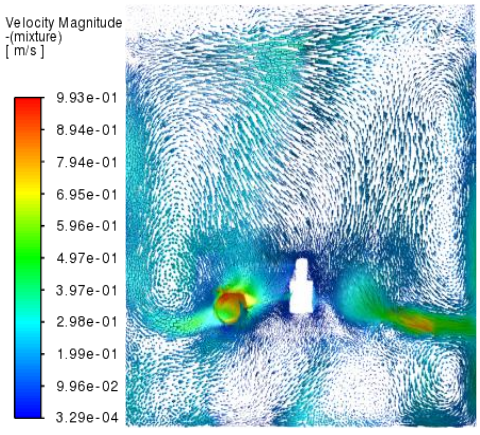

(a)

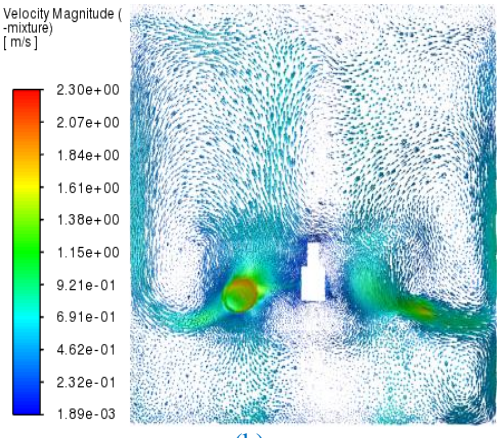

(b)

Fig. 16. Velocity field in the zy plane for Jet-1 (+15˚), with rotational speed (a) *N*=200 rpm, (b) *N*=400 rpm in water.

4 Conclusion

Analysis of the mixing process characteristics using numerical modelling and experimental (PIV, torque measurements) results show that the analyzed impellers – Jet-1 and Jet-2 - which have similar geometries, generate different flow fields under steady hydrodynamic conditions.

Both proposed Jet-1 and Jet-2 impeller types allow for reduced energy consumption, as evidenced by the low values of the calculated power number (N_P). However, a critical Reynolds number was identified beyond which the power number exhibits a pronounced initial decrease. The analyzed impellers constitute a promising alternative to conventional disk turbines and other bladed and bladeless mixers.

They are suitable for mixing fluids with a wide range of viscosities in cylindrical and cubic tanks.

It should be noted, however, that long operating time of the impeller when mixing highly viscous fluids may cause significant heat generation within the mixture.

The results indicate the need to develop a comprehensive parametric map and detailed process-characteristics data for both Jet-1 and Jet-2 impellers; this is another ongoing objective of our research.

Fundings. The work is supported by the program „Excellence Initiative – Research University" for the AGH University of Krakow, and was partly funded by AGH University of Krakow, Faculty of Civil Engineering and Resource Management (No.16.16.100.215)

Data availability statement. Data will be made available on request

Author contribution statement: A. Młynarczykowska: Writing – review & editing, Writing – original draft, Visualization, Validation, Supervision, Software, Resources, Project administration, Methodology, Investigation, Funding acquisition, Formal analysis, Data curation, Conceptualization. K. Zwolińska-Glądys: Writing – review & editing, Writing – original draft, Visualization, Software, Investigation, Formal analysis, Data curation. M. Borowski : Writing – review & editing, Supervision. M. Jaszczur: Writing – review & editing, Writing – original draft, Conceptualization, Software, Data curation Supervision.

References

1. A Bakker, K.J Myers, J.M. Smith, How to disperse gases in liquids. Chemical Engineering. 101, 98–104 (1994). http://www.bakker.org/cfm/publications/HowtoDisperse- GasesinLiquids1994.pdf.
2. K. Van't riet, J.M. Boom, J.M. Smith, Power consumption impeller coalescence and recirculation in aerated vessels. Trans. I. Chem E. 541, 124–131 (1976).
3. A.W. Nienow, Gas-Liquid Mixing Studies. A comparison of Rushton Turbines with some modern impellers. Trans.I. Chem. E. 74 A, 417–423 (1996). https://doi.org/10.1002/cjce.5450800409.
4. S. Nagata, Mixing Principals and Applications, (John Wiley & sons Halstead Press Tokyo Japan, 1975)
5. K Suzukawa, S Mochizukib, H. Osaka, Effect of the attack angle on the roll and trailing vortex structures in an agitated vessel with a paddle impeller. Chem. Engineer. Sci. 61, 2791–2798 (2006). DOI: http://dx.doi.org/10.1016/j.ces.2005.10.063
6. M. Ammar, W Chtourou, Z. Driss, M.S. Abid, Numerical investigation of turbulent flow generated in baffled stirred vessels equipped with three different turbines in one and two-stage system. Energy, 36, 5081–5093 (2011). http://dx.doi.org/10.1016/j.energy.2011.06.002.
7. T. Kumaresan, J.B. Joshi, Effect of impeller design on the flow pattern and mixing in stirred tanks. Chem. Eng. Sci. 1153, 173–193 (2006). https://doi.org/10.1016/j.cej.2005.10.002
8. Z. Driss, G .Bouzgarrou, W. Chtourou, H. Kchaou, M.S. Abid, Computational studies of the pitched blade turbines design effect on the stirred tank flow characteristics. European J. Mechanics B/Fluids. 29, 236–245 (2010). https://doi.org/10.1016/j.euromechfl u.2010.01.006.
9. D. Chapple, S. Kresta, A. Wall, A. Afcan, The effect of Impeller and Tank Geometry on Power Number for a pitched blade turbine. Chem. Engineer. Res. Design. 804, 364–372 (2002). http://dx.doi.org/10.1205/026387602317446407
10. H. Ameur, M. Bouzit, Numerical investigation of flow induced by a disc turbine in unbaffled stirred tank. Acta Sci. Tech. 35, 469–476 (2013). http://dx.doi.org/10.4025/actascitechnol.v35i3.15554
11. J. Aubin, P. Mavros, D. Fletcher, J. B. C. Xuereb, Effect of axial agitator configuration up-pumping down-pumping reverse rotation on flow patterns generated in stirred vessels. Chem. Engineer. Res. Design. 79, 845–856 (2001). https://doi.org/10.1205/02638760152721046
12. H. Ameur, Energy efficiency of different impellers in stirred tank reactors. Energy 93, 1980–1988 (2015). https://doi.org//10.1016/j.energy.2015.10.084.
13. B. Ben Amira, Z. Driss, M.S. Abid, PIV study of the turbulent flow in a stirred vessel equipped by an eight concave blades turbine. Fluid Mechanics. 12, 5–10 (2015). https://doi.org/10.11648/j.fm.20150102.11.
14. B. Ben Amira, Z. Driss, M.S. Abid, Experimental study of the up-pitching blade effect with a PIV application. Ocean Engineer. 102, 95–104 (2015). https://doi.org/10.1016/j.oceaneng.2015.08.063.
15. Z. Jing, G. Zhengming, B. Yuyun, Effects of the Blade Shape on the Trailing Vortices in Liquid Flow Generated by Disc Turbines. Chinese J. Chem. Engineer. 19(2), 232–242 (2011). https://doi.org/10.1016/S1004-9541(11)60160-2.
16. M. Jaszczur, A. Młynarczykowska, L. Demurtas, Effect of impeller design on power characteristics and Newtonian fluids mixing efficiency in a

mechanically agitated vessel at low Reynolds numbers. Energies **13**(3) 1-19, (2020). https://doi.org/10.3390/en13030640

17. M. Jaszczur, A. Młynarczykowska, A General Review of the Current Development of Mechanically Agitated Vessels. Processes **8**(8), 982 (2020). https://doi.org/10.3390/pr8080982
18. W. Zhang, Z. Gao, Q. Yang, S. Zhou, D. Xia, Study of Novel Punched-Bionic Impellers for High Efficiency and Homogeneity in PCM Mixing and Other Solid-Liquid Stirs. Appl. Sci. 11(21), 9883 (2021). https://doi.org/10.3390/app11219883
19. X. Zhan, B. Ye, B. Li, T. Shi, Continuous conveying and mixing characteristics of high-viscosity materials under acoustic vibration excitation. AIChE Journal. 18406 (2024). https://doi.org/10.1002/aic.18406
20. R. Liyanage, A. Russell, J.P. Crawshaw, S. Krevor, Direct experimental observations of the impact of viscosity contrast on convective mixing in a three-dimensional porous medium. Physics of Fluids 32, 056604 (2020). https://doi.org/10.1063/5.0006679
21. P. Prajapati, CFD Investigation of Mixing of Yield-Pseudoplastic Fluid with Anchor Impeller. PhD thesis, Ryerson University, Paper 1180 (2008).
22. A. Młynarczykowska, S. Ferrari, L. Demurtas, M. Jaszczur, An experimental investigation on the fluid flow mixing process in agitated vessel, in Proceedings of the EFM 2019 : Františkovy Lázně, Czech Republic, November 19th–22nd 2019, published: EPJ Web of Conferences 01040, 269, 1-6 (2022). https://doi.org/10.1051/epjconf/202226901040
23. A. Młynarczykowska, Mechanical Mixing in Technological Processes – Experimental Verification of Rotor Shape Prototyping. J. Polish Min. Eng. Soc. **1** (1), 177-182 (2025). https://doi.org/10.29227/IM-2025-01-23
24. K. Zwolińska-Glądys, A. Młynarczykowska, M. Jaszczur, M. Borowski, Mixing analysis in a stirred tank equipped with innovative impeller in Proceedings of the 15th International Conference on Computational Heat & Mass Transfer, Antalya, Turkiye, May 19-22 (2025), ID: 167
25. FlowMaster: Product Manual for DaVis 11; LaVision GmbH: Göttingen, Germany, 2025.
26. H, Singh, D.F. Fletcher, J.J. Nijdam, An assessment of different turbulence models for predicting flow in a baffled tank stirred with a Rushton turbine. Chem. Eng. Sci., **66(**23), 5976-5988 (2011). https://doi.org/10.1016/j.ces.2011.08.018
27. H. Patil, A.K. Patel, H.J. Pant, A.V. Vinod, CFD simulation model for mixing tank using multiple reference frame (MRF) impeller rotation, ISH J of Hydr. Eng., **2**, 971 (2018). https://doi.org/10.1080/09715010.2018.1535921
28. R.V. Calabrese, S.M. Kresta and M. Liu, Recognizing the 21 Most Influentila Contributions to Mixing Research, Chem. Eng. Progress, **110** (1), 20 – 29 (2014).